

A Unified Tensor Regression Framework for Calibrationless Dynamic, Multi-Channel MRI Reconstruction

Joshua D. Trzasko¹ and Armando Manduca¹
¹Mayo Clinic, Rochester, MN, United States

TARGET AUDIENCE: Magnetic resonance image (MRI) reconstruction developers.

PURPOSE: Advanced image reconstruction strategies often require explicit knowledge about the MRI acquisition system or target signal. For example, the GRAPPA [1] method for parallel MRI requires a kernel model of inter-coil k-space correlations that result from receiver sensitivity modulations; and kt-BLAST [2] requires a model of physiological bulk motion to perform dynamic MRI reconstruction. This information is typically obtained from an auxiliary scan or embedded reference signal, either of which necessitates prolonged scan duration. Error propagation also results when this information is presumed as exact during reconstruction. Recently, it has been shown that parallel and dynamic MRI reconstruction can each be formulated as a low-rank matrix regression problem whose only variable quantity is the target signal. Amongst other benefits, “calibrationless” parallel [3-5] and “training-free” dynamic [6-8] MRI reconstruction strategies offer improved sampling flexibility and statistical efficiency. In this work, we present a unifying tensor regression framework for calibrationless reconstruction of dynamic and multi-channel MRI data.

METHODS: The target dynamic multi-channel (2D or 3D) MRI signal, \mathbf{X} , can be described as a 3-way tensor with dimensions space, time, and coils (Fig. 1). Correspondingly, the observed k-space signal is $\mathbf{G} = A\{\mathbf{X}\} + \mathbf{Z}$, where $A\{\cdot\}$ is an undersampled Fourier operator that acts along only the spatial tensor dimension and \mathbf{Z} is complex Gaussian noise, and \mathbf{X} can be estimated from \mathbf{G} via penalized regression: $[\hat{\mathbf{X}}] = \arg \min \{P(\mathbf{X}) + \|\mathbf{A}\{\mathbf{X}\} - \mathbf{G}\|_F^2\}$, where $\|\cdot\|_F$ is the Frobenius norm and $P(\cdot)$ is a penalty functional. As with matrices, $P(\cdot)$ can be defined so as to promote low-rankness. For tensors, a natural penalty is $P(\mathbf{X}) = \sum_{i=1}^3 \lambda_i \text{rank}(\mathbf{X}_{(i)})$, the weighted sum of the n-rank vector [9,10], where $\mathbf{X}_{(i)}$ is the i^{th} unfolding. However, rank is nonconvex, and minimization of spectral functionals of highly anisotropic matrices can face degree-of-freedom limitations [8]. Thus, we let $P(\mathbf{X}) = \sum_{i=1}^3 \lambda_i \sum_{b \in \Omega} \|R_b\{\mathbf{X}_{(i)}\}\|_*$, where $\|\cdot\|_*$ is the nuclear norm (convex envelope of rank), $R_b\{\mathbf{X}\}$ extracts a spatial submatrix of $\mathbf{X}_{(i)}$, and Ω is a set of blocks that uniformly tiles the tensor spatial dimension. We also know from [4,7] that sparsity and low-rankness are complementary objectives, and so finally consider:

$$[\hat{\mathbf{X}}] = \arg \min \{P_{\text{SPARSE}}(\mathbf{X}) + \sum_{i=1}^3 \lambda_i \sum_{b \in \Omega} \|R_b\{\mathbf{X}_{(i)}\}\|_* + \|\mathbf{A}\{\mathbf{X}\} - \mathbf{G}\|_F^2\}, \quad (1)$$

where $P_{\text{SPARSE}}(\cdot)$ promotes image sparsity. For single-coil dynamic MRI reconstruction, (1) exactly resorts to the matrix model defined in [8], and to those from [6,7] when Ω comprises a single full-sized block. For static multi-channel MRI reconstruction, (1) yields CLEAR [4]. Thus, (1) unifies existing image-domain low-rank matrix methods for dynamic and parallel MRI as well as generalizes and extends them. The problem in (1) can be efficiently solved via alternating direction method of multipliers (ADMM) [11], with constraint set $\{\mathbf{X}_{(1)} = \mathbf{Y}_1, \mathbf{X}_{(2)} = \mathbf{Y}_2, \mathbf{X}_{(3)} = \mathbf{Y}_3, \mathbf{X} = \mathbf{Z}\}$ and augmented Lagrangian functional

$$[\hat{\mathbf{X}}] = \arg \min \{P_{\text{SPARSE}}(\mathbf{Z}) + \sum_{i=1}^3 \lambda_i \sum_{b \in \Omega} \|R_b\{\mathbf{Y}_i\}\|_* + \|\mathbf{A}\{\mathbf{X}\} - \mathbf{G}\|_F^2\}. \quad (2)$$

RESULTS: Fig. 2 shows example results for a 144x144x19 short-axis cine cardiac exam (GE Signa v.14.0, 1.5 T, FIESTA, FA=50°, TR/TE=2.8/1.2 ms, 8 channel upper body coil) that was retrospectively 4x variable-density Poisson Disk undersampled in k-t space [12]. For (1), we define $P_{\text{SPARSE}}(\cdot)$ as the joint sparsity (across coils) generalization of the kt-SPARSE [13] penalty: $P_{\text{SPARSE}}(\mathbf{Z}) = \lambda_0 \|\Psi\{\mathbf{Z}\}\|_{(3)}\|_{1,2}$, where $\Psi\{\cdot\}$ is temporal Fourier transform. Minimization of (1) via ADMM using only the tensor n-rank penalty, and with both the n-rank and sparsity, was executed. Regularization parameters were manually tuned. For the tensor penalty, Ω comprised the set of disjoint 6x6 spatial blocks. Each 50 iteration Matlab reconstruction required only a few minutes of computation on a dual 2.93 GHz 6-core machine with 24 GB MHz memory. Sliding window reconstruction was also performed.

DISCUSSION: As expected, sliding window reconstruction exhibits marked blurring in the phase encoded direction as well as residual aliasing artifact. Standalone low n-rank tensor reconstruction effectively suppresses this aliasing and recovers dominant morphological features. Incorporating the auxiliary sparsity penalty complementarily improves recovery of tissue morphology (green arrow) as well as fine anatomical structure (red arrow). These observations mirror those previously seen in [7] for low-rank matrix recovery of dynamic MRI series.

CONCLUSION: The low n-rank tensor approach provides a unifying image-domain foundation for high-quality calibrationless parallel and dynamic MRI reconstruction.

REFERENCES: [1] Griswold et al., MRM 2002;47:1202-10. [2] Tsao et al., MRM 2003;50:1031-42. [3] Lustig et al., ISMRM 2010:2870. [4] Trzasko and Manduca, ISMRM 2012:517. [5] Otazo et al., ISMRM 2012:4248. [6] Haldar and Liang, ISBI 2010:716-9. [7] Lingala et al., IEEE TMI 2011;30:1042-52. [8] Trzasko and Manduca, ISMRM 2011:4371. [9] Kolda and Bader, SIAM Rev 2009;51:455-500. [10] Gandy et al., Inv Prob 2011;27:1-19. [11] Ramani and Fessler, IEEE TMI 2011;30:694-706. [12] Lai et al., ISMRM 2010:482. [13] Lustig et al., ISMRM 2006:2420.

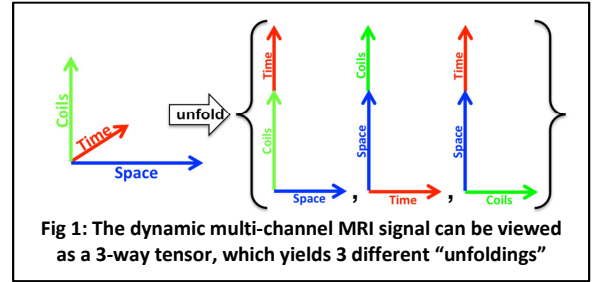


Fig 1: The dynamic multi-channel MRI signal can be viewed as a 3-way tensor, which yields 3 different “unfoldings”

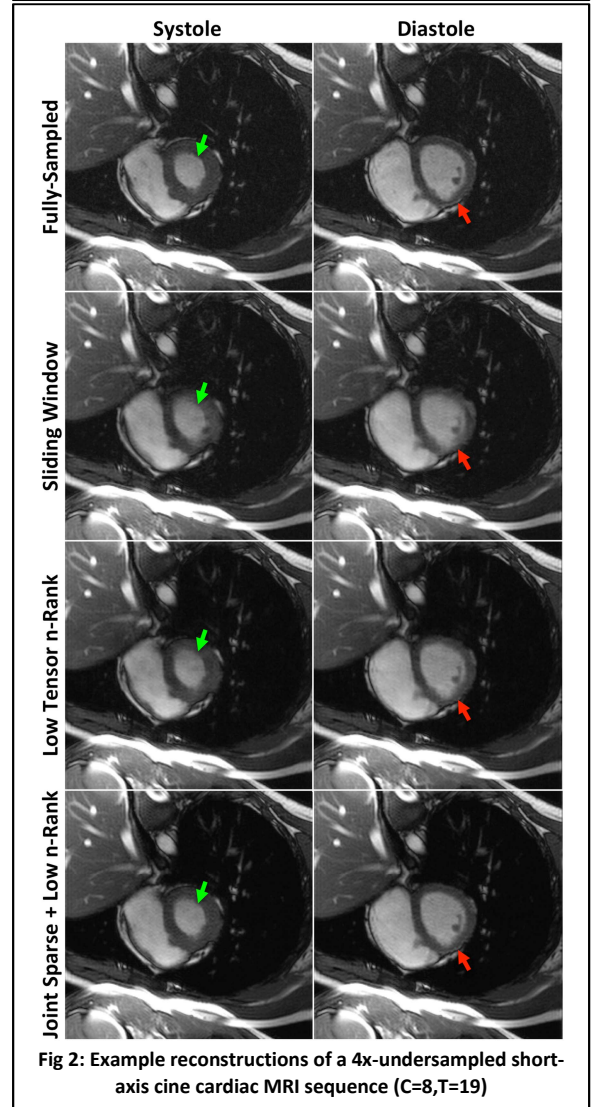


Fig 2: Example reconstructions of a 4x-undersampled short-axis cine cardiac MRI sequence (C=8,T=19)